Acta Poloniae Pharmaceutica – Drug Research, Vol. 79 No. 5 pp. 643-659, 2022
DOI: 10.32383/appdr/157503
Received 3 August 2022, Received in revised form 13 November 2022, Accepted 15 December 2022
ISSN 2353-5288
Polish Pharmaceutical Society

**DRUG SYNTHESIS**

# SYNTHESIS AND STRUCTURAL CHARACTERIZATION OF NOVEL 2-PYRAZOLINE DERIVATIVES: EVALUATION OF THEIR ANTIPROLIFERATIVE ACTIVITY AND FLUORESCENCE PROPERTIES

ZEFINE UGRAS[1,2], FATIH TOK[2], EMINE SALVA[3], GOZDE ULTAV[3], and BEDIA KOCYIGIT-KAYMAKCIOGLU[2,*]

[1]Institute of Health Sciences, Marmara University, Dragos, 34865 Kartal, Istanbul
[2]Department of Pharmaceutical Chemistry, Faculty of Pharmacy, Marmara University, 34854 Maltepe, Istanbul
[3]Department of Pharmaceutical Biotechnology, Faculty of Pharmacy, Inönü University, 44280 Battalgazi, Malatya

**Abstract:** In this study, a series of novel 2-pyrazoline derivatives were synthesized and their structures were established by using spectral methods. The antiproliferative activities of compounds were investigated against human cell lines A-549 and MCF-7 by MTT assay and L-929 (mouse normal fibroblast) cell cytotoxicity was also examined. Apoptotic effects of the compounds in breast and lung cancer cells were assessed by Annexin V-FITC apoptosis assay using flow cytometry. The antiproliferative effect on lung carcinoma of the synthesized compounds was higher than breast carcinoma. Moreover, it was observed that none of the synthesized compounds have cytotoxic activity in healthy cells. Flow cytometry studies have shown that compounds induced apoptosis at high concentrations. Additionally, fluorescence cell imaging studies were performed for the first time in A-549 and MCF-7 cancer cell lines to determine the potential of the biosensor compounds by fluorescence microscopy. Compounds **4b, 4d, 4e,** and **4f** showed fluorescence properties by considering microscopic imaging.

**Keywords:** synthesis, pyrazoline, structural characterization, cytotoxic, fluorescent imaging.

Fluorescent probes are used in many fields such as genomics and proteogenomics, medical diagnoses like monitoring DNA and RNA abundance, localization and dynamics of nucleic acids, drug discovery, and microscopy (1, 2). Fluorescent probes are important molecular tools for analytical and optical imaging due to their high sensitivity, specificity, rapid response, and simple applicability (3). To date, countless synthetic fluorescent probes were designed, synthesized, and widely used in the recognition of biomolecules (anions, enzymes, reactive oxygen, nıtrogen, and sulfur species (4). Some exogenous fluorophores such as fluorescein and indocyanine green (ICG) which are approved FDA (Food and Drug Administration) are used to analyze and characterize tissues.

Pyrazoline scaffold has a non-toxic bioactive property and is well known as a fluorescent probe due to its charge transfer character besides playing an important role in biological activities such as antibacterial (5), antidiabetic (6), antifungal (7), anti-inflammatory (8), anticancer (9), anticonvulsant (10), antinociceptive (11), antioxidant (12) and antipyretic (13). Pyrazolines attract great attention due to their strong fluorescence properties, good membrane permeability, low toxicity, and simple synthesis methods (14-16).

Intramolecular charge transfer (ICT) change is formed in the pyrazoline structure as a result of excitation with light. It occurs from the nitrogen atom in the 1st position to the nitrogen atom in the 2nd position and the carbon atom in the 3rd position, which can cause a conformational change in the molecular structure. Molecular planarity is required for fluorescence activity (17).

It is known that the pyrazoline ring, which carries at least two aryl substituents in the 1st and 3rd positions, exhibits a strong fluorescence activity. With the formation of the pyrazoline ring, the ring has a planar structure with the effect of carbon atoms in the 4th and 5th positions, and the aromatic rings in the 1st and 3rd positions interact through

* Corresponding author: e-mail: bkaymakcioglu@marmara.edu.tr

mesomeric and canonical forms. The presence of styryl or heterocyclic structures instead of aromatic rings does not have a significant effect on fluorescence properties (18).

In this study, some novel 2-pyrazoline derivatives carrying piperidine rings were synthesized as a result of a cyclo condensation reaction between chalcone and hydrazine derivatives. The structures were evaluated by spectral characterization. The fluorescence properties of the compounds were evaluated by fluorescence spectroscopy besides the cytotoxic activities of the compounds in cancer and fibroblast cell lines. Further, the SwissADME program was utilized to determine the pharmacokinetic properties and bioavailability of the compounds.

## EXPERIMENTAL

All the reagents, chemicals, and solvents were obtained from Sigma Aldrich (St. Louis, MO, USA), and Merck (Darmstadt, Germany) and used without further purification. The process of reactions was monitored by thin-layer chromatography (TLC) using silica gel (Kieselgel 60, F254) and aluminum sheets (Merck) under a UV lamp. Petroleum ether : ethyl acetate (10 : 90) was used as a solvent system. Melting points of the synthesized compounds were measured by using the Schmelzpunktbestimmer SMP II apparatus. HMBC, $^{1}$H-NMR, and $^{13}$C-NMR spectra of products were recorded by UXNMR, Bruker Analytische Messtechnik GmbH (400 Hz), and Varian Mercury (Agilent) FT (400 Hz) spectrometer using tetramethylsilane (TMS) as an internal reference. DMSO-$d_6$ was used as a solvent in nuclear magnetic spectra. All chemical shift values of the compounds were expressed as δ in ppm and coupling constants *(J)* values were given in Hertz (Hz). Infrared Spectra (IR) values were obtained by operating Shimadzu FTIR 8400 S Spectrometer. The mass spectra were recorded on the Waters Micromass ZQ LC-MS spectrometer (Waters Corporation, Milford, MA) by using the ESI(+) method.

### Chemistry

The 4-(4-methylpiperidine-1-yl)benzaldehyde derivative was obtained by referring to the synthesis method in the literature (19).

### The general synthesis method of chalcone derivatives

Appropriate compounds were synthesized by mixing an equivalent amount of benzaldehyde (1 mmol) and a substituted ketone (1 mmol) with 3 equivalents of NaOH in methanol at room temperature on a magnetic stirrer. The crude products were purified by crystallization from ethanol (20).

#### *3-[4-(4-Methylpiperidin-1-yl)phenyl]-1-phenylprop-2-en-1-one (1a)*

Yield 86%; yellow solid; m.p. 144.3-144.9°C; $^{1}$H NMR (400 MHz, DMSO-$d_6$): $\delta$ 0.90 (3H, d, $J$ = 6.5 Hz, $CH_3$), 1.15 (2H, q, piperidine -$CH_2$- protons), 1.55 (1H, m, piperidine -CH- protons), 1.67 (2H, m, piperidine -$CH_2$- protons), 2.78 (2H, t, piperidine N-$CH_2$- protons), 3.86 (2H, d, piperidine N-$CH_2$- protons), 6.93-8.11 (11H, m, -CH=CH- and Ar-H); IR ($\nu_{max}$) cm$^{-1}$: 3055 (aromatic C=C-H), 2949 (chalcone C=C-H g.b.), 2866 (aliphatic C-H), 1651 (C=O), 1568, 1514 (C=C), 1288 (C-N).

#### *1-(5-Chlorothiophen-2-yl)-3-[4-(4-methylpiperidin-1-yl)phenyl]prop-2-en-1-one (1b)*

Yield 88%; orange solid; m.p. 149.9-150.6°C; $^{1}$H NMR (400 MHz, DMSO-$d_6$): $\delta$ 0.91 (3H, d, $J$ = 6.5 Hz, $CH_3$), 1.15 (2H, q, piperidine -$CH_2$- protons), 1.56 (1H, m, piperidine -CH- protons), 1.67 (2H, m, piperidine -$CH_2$- protons), 2.79 (2H, t, piperidine N-$CH_2$- protons), 3.88 (2H, d, piperidine N-$CH_2$- protons), 6.95-8.17 (8H, m, -CH=CH- and Ar-H); IR ($\nu_{max}$) cm$^{-1}$: 3096 (aromatic C=C-H), 2951 (chalcone C=C-H g.b.), 2835 (aliphatic C-H), 1633 (C=O), 1570, 1514 (C=C), 1257 (C-N).

#### *1-(Furan-2-yl)-3-[4-(4-methylpiperidin-1-yl) phenyl]prop-2-en-1-one (1c)*

Yield 86%; yellow solid; m.p. 147.5-148.3°C; $^{1}$H NMR (400 MHz, DMSO-$d_6$): $\delta$ 0.92 (3H, d, $J$ = 6.5 Hz, $CH_3$), 1.17 (2H, q, piperidine -$CH_2$- protons), 1.57 (1H, m, piperidine -CH- protons), 1.68 (2H, m, piperidine -$CH_2$- protons), 2.80 (2H, t, piperidine N-$CH_2$- protons), 3.89 (2H, m, piperidine N-$CH_2$- protons), 6.76-8.03 (9H, m, -CH=CH- and Ar-H); IR ($\nu_{max}$) cm$^{-1}$: 3068 (aromatic C=C-H), 2949 (chalcone C=C-H g.b.), 2812 (aliphatic C-H), 1645 (C=O), 1573, 1552 (C=C), 1232 (C-N).

#### *1-(5-Bromothiophen-2-yl)-3-[4-(4-methylpiperidin-1-yl)phenyl]prop-2-en-1-one (1d)*

Yield 95%; orange solid; m.p. 149.0-149.5°C; $^{1}$H NMR (400 MHz, DMSO-$d_6$): $\delta$ 0.92 (3H, d, $J$ = 6.5 Hz, $CH_3$), 1.16 (2H, q, piperidine -$CH_2$- protons), 1.57 (1H, m, piperidine -CH- protons), 1.69 (2H, m, piperidine -$CH_2$- protons), 2.81 (2H, t, piperidine N-$CH_2$- protons), 3.90 (2H, d, piperidine N-$CH_2$- protons), 6.96-8.12 (8H, m, -CH=CH- and

Ar-H); IR ($\nu_{max}$) $cm^{-1}$: 3086 (aromatic C=C-H), 2919 (chalcone C=C-H g.b.), 2810 (aliphatic C-H), 1635 (C=O), 1573, 1556 (C=C), 1303 (C-N).

***3-[4-(4-Methylpiperidin-1-yl)phenyl]-1-(thiophen-2-yl)prop-2-en-1-one (1e)***

Yield 91%; yellow solid; m.p. 171.1-171.8°C; $^1$H NMR (400 MHz, DMSO-$d_6$): δ 0.93 (3H, d, J = 6.5 Hz, $CH_3$), 1.17 (2H, q, piperidine -$CH_2$- protons), 1.59 (1H, m, piperidine -CH- protons), 1.68 (2H, m, piperidine -$CH_2$- protons), 2.80 (2H, t, piperidine N-$CH_2$- protons), 3.89 (2H, d, piperidine N-$CH_2$- protons), 6.97-8.26 (9H, m, -CH=CH- and Ar-H); IR ($\nu_{max}$) $cm^{-1}$: 3093 (aromatic C=C-H), 2912 (chalcone C=C-H g.b.), 2831 (aliphatic C-H), 1637 (C=O), 1573, 1514 (C=C), 1309 (C-N).

***3-[4-(4-Methylpiperidin-1-yl)phenyl]-1-(5-methylthiophen-2-yl)prop-2-en-1-one (1f)***

Yield 83%; orange solid; m.p. 165.1-165.9°C; $^1$H NMR (400 MHz, DMSO-$d_6$): $\delta$ 0.92 (3H, d, $J$ = 6.5 Hz, $CH_3$), 1.17 (2H, q, piperidine -$CH_2$- protons), 1.59 (1H, m, piperidine -CH- protons), 1.68 (2H, m, piperidine -$CH_2$- protons), 2.80 (2H, t, piperidine N-$CH_2$- protons), 3.89 (2H, d, piperidine N-$CH_2$- protons), 2.53 (3H, s, $CH_3$), 6.93-8.07 (8H, m, -CH=CH- and Ar-H); IR ($\nu_{max}$) $cm^{-1}$: 3066 (aromatic C=C-H), 2918 (chalcone C=C-H g.b.), 2835 (aliphatic C-H), 1633 (C=O), 1572, 1514 (C=C), 1309 (C-N).

**The general synthesis method of 2-pyrazoline derivatives**

A mixture of chalcone derivative (0.01 mol) and phenylhydrazine hydrochloride (0.04 mol) in acetic acid (20 mL) was heated for 10-11 hours. The crude solution was poured into ice water. The precipitated solid product was filtered and crystallized from ethanol to give the pure product (21).

***1-[4-(1,3-Diphenyl-4,5-dihydro-1H-pyrazol-5-yl) phenyl]-4-methylpiperidine (2a)***

Yield 76%; white solid; m.p. 151.5-152.3°C; $^1$H NMR (400 MHz, DMSO-$d_6$): $\delta$ 0.90 (3H, d, $J$ = 6.5 Hz, $CH_3$), 1.18 (2H, q, piperidine -$CH_2$- protons), 1.45 (1H, m, piperidine -CH- protons), 1.64 (2H, m, piperidine -$CH_2$- protons), 2.58 (2H, m, piperidine N-$CH_2$- protons), 3.04 (1H, dd, *Jax* = 6.4 Hz, *Jab* = 17.4 Hz, Ha), 3.58 (2H, m, piperidine N-$CH_2$- protons), 3.83 (1H, dd, *Jbx* = 12.1 Hz, *Jab* = 17.4 Hz, Hb), 5.33 (1H, dd, *Jax* = 6.4 Hz, *Jbx* = 12.1 Hz, Hx), 6.69–7.76 (14H, m, Ar-H); $^{13}$C NMR (100 MHz, DMSO-*d6*): δ 22.2, 30.6, 34.0, 43.4, 49.1, 49.2, 63.2, 113.4, 116.5, 118.9, 126.1, 127.0, 129.1, 129.3, 132.5, 132.9, 144.8, 147.6, 151.1; IR ($\nu_{max}$) $cm^{-1}$: 3026 (aromatic C=C-H), 2920 (aliphatic C-H), 1597 (C=N), 1492 (C=C), 1222 (C-N); MS (ESI+): m/z = 396.78 $[M+H]^+$ (Calcd for C27H29N3: m/z = 395.24 $[M^+]$).

***1-{4-[1-Phenyl-3-(5-chlorothiophen-2-yl)-4,5-dihydro-1H-pyrazol-5-yl]phenyl}-4-methylpiperidine (2b)***

Yield 61%; orange solid; m.p. 114.1-114.7 C; $^1$H NMR (400 MHz, DMSO-$d_6$): $\delta$ 0.90 (3H, d, $J$ = 6.5 Hz, $CH_3$), 1.17 (2H, q, piperidine -$CH_2$- protons), 1.44 (1H, m, piperidine -CH- protons), 1.63 (2H, m, piperidine -$CH_2$- protons), 2.57 (2H, m, piperidine N-$CH_2$- protons), 3.04 (1H, dd, *Jax* = 6.3 Hz, *Jab* = 17.3 Hz, Ha), 3.58 (2H, m, piperidine N-$CH_2$- protons), 3.79 (1H, dd, *Jbx* = 12.1 Hz, *Jab* = 17.3 Hz, Hb), 5.36 (1H, dd, *Jax* = 6.3 Hz, *Jbx* = 12.1 Hz, Hx), 6.69–7.15 (11H, m, Ar-H); $^{13}$C NMR (100 MHz, DMSO-*d6*): δ 22.2, 30.5, 33.9, 43.4, 49.1, 63.4, 113.4, 116.4, 119.2, 126.9, 127.2, 128.1, 129.2, 129.3, 131.8, 135.4, 143.3, 144.2, 151.0; IR ($\nu_{max}$) $cm^{-1}$: 3032 (aromatic C=C-H), 2922 (aliphatic C-H), 1595 (C=N), 1496 (C=C), 1228 (C-N); MS (ESI+): m/z = 436.73 $[M+H]^+$(Calcd for C25H26ClN3S: m/z = 435.15 $[M^+]$).

***1-{4-[1-Phenyl-3-(furan-2-yl)-4,5-dihydro-1H-pyrazol-5-yl]phenyl}-4-methylpiperidine (2c)***

Yield 65%; brown solid; m.p. 179.9-181.6°C; $^1$H NMR (400 MHz, DMSO-$d_6$): $\delta$ 0.90 (3H, d, $J$ = 6.5 Hz, $CH_3$), 1.18 (2H, m, piperidine -$CH_2$- protons), 1.44 (1H, m, piperidine -CH- protons), 1.64 (2H, m, piperidine -$CH_2$- protons), 2.57 (2H, m, piperidine N-$CH_2$- protons), 2.94 (1H, dd, *Jax* = 6.0 Hz, *Jab* = 17.2 Hz, Ha), 3.58 (2H, m, piperidine N-$CH_2$- protons), 3.76 (1H, dd, *Jbx* = 12.0 Hz, *Jab* = 17.2 Hz, Hb), 5.31 (1H, dd, *Jax* = 6.0 Hz, *Jbx* = 12.0 Hz, Hx), 6.59–7.78 (12H, m, Ar-H); $^{13}$C NMR (100 MHz, DMSO-*d6*): δ 22.2, 30.6, 33.9, 43.3, 49.1, 62.5, 111.1, 112.4, 113.4, 118.9, 126.9, 129.2, 132.0, 139.6, 144.5, 144.6, 148.0, 151.0; IR ($\nu_{max}$) $cm^{-1}$: 3030 (aromatic C=C-H), 2914 (aliphatic C-H), 1597 (C=N), 1500 (C=C), 1230 (C-N). MS (ESI+): m/z = 386.76 $[M+H]^+$ (Calcd for $C_{25}H_{27}N_3O$: m/z = 385.22 $[M^+]$).

***1-{4-[1-Phenyl-3-(5-bromothiophen-2-yl)-4,5-dihydro-1H-pyrazol-5-yl]phenyl}-4-methylpiperidine (2d)***

Yield 76%; green solid; m.p. 135.4-136.0°C; $^1$H NMR (400 MHz, DMSO-$d_6$): $\delta$ 0.90 (3H, d, $J$ = 6.5 Hz, $CH_3$), 1.17 (2H, q, piperidine -$CH_2$- protons), 1.44 (1H, m, piperidine -CH- protons), 1.64 (2H, m, piperidine -$CH_2$- protons), 2.59 (2H,

m, piperidine N-$CH_2$- protons), 3.02 (1H, dd, *Jax* = 6.2 Hz, *Jab* = 17.3 Hz, Ha), 3.58 (2H, m, piperidine N-$CH_2$- protons), 3.79 (1H, dd, *Jbx* = 12.1 Hz, *Jab* = 17.3 Hz, Hb), 5.36 (1H, dd, *Jax* = 6.2 Hz, *Jbx* = 12.1 Hz, Hx), 6.68–7.20 (11H, m, Ar-H); $^{13}$C NMR (100 MHz, DMSO-*d6*): $\delta$ 22.1, 30.5, 33.9, 43.5, 49.1, 63.4, 112.9, 113.5, 116.6, 119.2, 127.0, 128.1, 129.3, 131.6, 138.0, 143.2, 144.2; IR ($\nu_{max}$) $cm^{-1}$: 3032 (aromatic C=C-H), 2920 (aliphatic C-H), 1595 (C=N), 1500 (C=C), 1226 (C-N). MS (ESI+): m/z = 480.69 $[M+H]^+$(Calcd for $C_{25}H_{26}BrN_3S$: m/z = 479.10 $[M^+]$).

***1-{4-[1-Phenyl-3-(thiophen-2-yl)-4,5-dihydro-1H-pyrazol-5-yl]phenyl}-4-methylpiperidine (2e)***

Yield 75%; cream color solid; m.p. 186.6-187.2°C; $^1$H NMR (400 MHz, DMSO-$d_6$): $\delta$ 0.89 (3H, d, *J* = 6.5 Hz, $CH_3$), 1.17 (2H, m, piperidine -$CH_2$- protons), 1.44 (1H, m, piperidine -CH- protons), 1.64 (2H, m, piperidine -$CH_2$- protons), 2.59 (2H, m, piperidine N-$CH_2$- protons), 3.05 (1H, dd, *Jax* = 6.2 Hz, *Jab* = 17.3 Hz, Ha), 3.58 (2H, m, piperidine N-$CH_2$- protons), 3.83 (1H, dd, *Jbx* = 12.0 Hz, *Jab* = 17.3 Hz, Hb), 5.33 (1H, dd, *Jax* = 6.2 Hz, *Jbx* = 12.0 Hz, Hx), 6.66–7.57 (12H, m, Ar-H); $^{13}$C NMR (100 MHz, DMSO-$d_6$): 22.2, 30.6, 34.0, 44.2, 49.1, 63.2, 113.4, 116.5, 118.9, 127.0, 127.7, 128.2, 129.3, 132.1, 136.3, 144.0, 144.5, 151.0; IR ($\nu_{max}$) $cm^{-1}$: 3032 (aromatic C=C-H), 2914 (aliphatic C-H), 1597 (C=N), 1500 (C=C), 1226 (C-N). MS (ESI+): m/z = 402.76 $[M+H]^+$ (Calcd for $C_{25}H_{27}N_3S$: m/z = 401.19 $[M^+]$).

***1-{4-[3-(5-methylthiophen-2-yl)-1-phenyl-4,5-dihydro-1H-pyrazol-5-yl]phenyl}-4-methyl piperidine (2f)***

Yield 90%; yellow solid; m.p. 174.6-175.4°C; $^1$H NMR (400 MHz, DMSO-$d_6$): $\delta$ 0.88 (3H, d, *J* = 6.5 Hz, $CH_3$), 1.16 (2H, m, piperidine -$CH_2$- protons), 1.44 (1H, m, piperidine -CH- protons), 1.63 (2H, m, piperidine -$CH_2$- protons), 2.44 (3H, s, $CH_3$), 2.55 (2H, t, piperidine N-$CH_2$- protons), 2.98 (1H, dd, *Jax* = 6.2 Hz, *Jab* = 17.2 Hz, Ha), 3.57 (2H, m, piperidine N-$CH_2$- protons), 3.77 (1H, dd, *Jbx* = 12.0 Hz, *Jab* = 17.2 Hz, Hb), 5.22 (1H, dd, *Jax* = 6.2 Hz, *Jbx* = 12.0 Hz, Hx), 6.65–7.20 (11H, m, Ar-H); $^{13}$C NMR (100 MHz, DMSO-$d_6$): $\delta$ 15.7, 22.2, 30.6, 34.0, 44.0, 49.1, 63.2, 113.3, 116.4, 118.7, 126.5, 126.9, 127.9, 129.2, 144.6; IR ($\nu_{max}$) $cm^{-1}$: 3024 (aromatic C=C-H), 2910 (aliphatic C-H), 1597 (C=N), 1499 (C=C), 1294 (C-N). MS (ESI+): m/z = 416.75 $[M+H]^+$(Calcd for $C_{26}H_{29}N_3S$: m/z = 415.21 $[M^+]$).

***1-{4-[1-(4-Chlorophenyl)-3-phenyl-4,5-dihydro-1H-pyrazol-5-yl]phenyl}-4-methylpiperidine (3a)***

Yield 76%; orange solid; m.p. 122.3-123.0°C; $^1$H NMR (400 MHz, DMSO-$d_6$): $\delta$ 0.91 (3H, d, *J* = 6.5 Hz, $CH_3$), 1.17 (2H, q, piperidine -$CH_2$- protons), 1.44 (1H, m, piperidine -CH- protons), 1.66 (2H, m, piperidine -$CH_2$- protons), 2.58 (2H, m, piperidine N-$CH_2$- protons), 3.09 (1H, dd, *Jax* = 6.0 Hz, *Jab* = 17.5 Hz, Ha), 3.61 (2H, m, piperidine N-$CH_2$- protons), 3.87 (1H, dd, *Jbx* = 12.1 Hz, *Jab* = 17.5 Hz, Hb), 5.38 (1H, dd, *Jax* = 6.0 Hz, *Jbx* = 12.1 Hz, Hx), 6.97–7.75 (13H, m, Ar-H); $^{13}$C NMR (100 MHz, DMSO-*d6*): $\delta$ 22.2, 30.6, 33.3, 43.5, 49.1, 63.0, 114.8, 116.5, 122.3, 126.2, 127.0, 129.0, 131.8, 132.6, 143.5, 148.4, 151.0; IR ($\nu_{max}$) $cm^{-1}$: 2920 (aromatic C=C-H), 2808 (aliphatic C-H), 1597 (C=N), 1489 (C=C), 1323 (C-N). MS (ESI+): m/z = 430.78 $[M+H]^+$ (Calcd for $C_{27}H_{28}ClN_3$: m/z = 429.20 $[M^+]$).

***1-{4-[1-(4-Chlorophenyl)-3-(5-chlorothiophen-2-yl)-4,5-dihydro-1H-pyrazol-5-yl]phenyl}-4-methylpiperidine (3b)***

Yield 72%; orange solid; m.p. 111.5-112.0 °C; $^1$H NMR (400 MHz, DMSO-$d_6$): $\delta$ 0.88 (3H, d, *J* = 6.5 Hz, $CH_3$), 1.17 (2H, m, piperidine -$CH_2$- protons), 1.44 (1H, m, piperidine -CH- protons), 1.63 (2H, m, piperidine -$CH_2$- protons), 2.56 (2H, m, piperidine N-$CH_2$- protons), 3.04 (1H, dd, *Jax* = 5.9 Hz, *Jab* = 17.4 Hz, Ha), 3.57 (2H, m, piperidine N-$CH_2$- protons), 3.79 (1H, dd, *Jbx* = 12.1 Hz, *Jab* = 17.4 Hz, Hb), 5.38 (1H, dd, *Jax* = 5.9 Hz, *Jbx* = 12.1 Hz, Hx), 6.82–7.19 (10H, m, Ar-H); $^{13}$C NMR (100 MHz, DMSO-*d6*): $\delta$ 22.2, 30.5, 33.9, 43.5, 49.1, 63.3, 114.9, 116.5, 122.7, 127.0, 127.7, 128.2, 129.1, 129.6, 131.4, 135.1, 143.0, 144.1, 151.0; IR ($\nu_{max}$) $cm^{-1}$: 3032 (aromatic C=C-H), 2916 (aliphatic C-H), 1595 (C=N), 1489 (C=C), 1384 (C-N). MS (ESI+): m/z = 470.69 $[M+H]^+$ (Calcd for $C_{25}H_{25}Cl_2N_3S$: m/z = 469.11 $[M^+]$).

***1-{4-[1-(4-Chlorophenyl)-3-(furan-2-yl)-4,5-dihydro-1H-pyrazol-5-yl]phenyl}-4-methylpiperidine (3c)***

Yield 60%; brown solid; m.p. 150.1-150.9°C; $^1$H NMR (400 MHz, DMSO-$d_6$): $\delta$ 0.93 (3H, d, *J* = 6.5 Hz, $CH_3$), 1.18 (2H, m, piperidine -$CH_2$- protons), 1.47 (1H, m, piperidine -CH- protons), 1.68 (2H, m, piperidine -$CH_2$- protons), 2.60 (2H, m, piperidine N-$CH_2$- protons), 2.99 (1H, dd, *Jax* = 5.7 Hz, *Jab* = 17.3 Hz, Ha), 3.60 (2H, m, piperidine N-$CH_2$- protons), 3.80 (1H, dd, *Jbx* = 11.9 Hz, *Jab* = 17.3 Hz, Hb), 5.37 (1H, dd, *Jax* = 5.7 Hz, *Jbx* = 11.9 Hz, Hx), 6.62–7.82 (11H, m, Ar-H); $^{13}$C NMR (100 MHz, DMSO-$d_6$): $\delta$ 22.1, 30.5, 33.9, 43.4, 49.1, 62.5, 11.5, 112.5, 114.8, 116.5, 122.4, 127.0, 129.0, 131.4, 140.4,

143.3, 144.8, 147.8; IR ($\nu_{max}$) $cm^{-1}$: 3032 (aromatic C=C-H), 2922 (aliphatic C-H), 1599 (C=N), 1494 (C=C), 1230 (C-N). MS (ESI+): m/z = 420.75 $[M+H]^+$ (Calcd for $C_{25}H_{26}ClN_3O$: m/z = 419.18 $[M^+]$).

***1-{4-[3-(5-Bromothiophen-2-yl)-1-(4-chlorophenyl)-4,5-dihydro-1H-pyrazol-5-yl] phenyl}-4-methylpiperidine (3d)***

Yield 91%; yellow solid; m.p. 159.2-160.1°C; $^1$H NMR (400 MHz, DMSO-$d_6$): $\delta$ 0.91 (3H, d, $J$ = 6.5 Hz, $CH_3$), 1.18 (2H, m, piperidine -$CH_2$- protons), 1.46 (1H, m, piperidine -CH- protons), 1.67 (2H, m, piperidine -$CH_2$- protons), 2.58 (2H, m, piperidine N-$CH_2$- protons), 3.08 (1H, dd, *Jax* = 5.8 Hz, *Jab* = 17.4 Hz, Ha), 3.61 (2H, m, piperidine N-$CH_2$- protons), 3.83 (1H, dd, *Jbx* = 12.0 Hz, *Jab* = 17.4 Hz, Hb), 5.41 (1H, dd, *Jax* = 5.8 Hz, *Jbx* = 12.0 Hz, Hx), 6.84–7.24 (10H, m, Ar-H); $^{13}$C NMR (100 MHz, DMSO-$d_6$): $\delta$ 22.2, 30.6, 33.9, 43.6, 49.0, 49.0, 63.2, 113.3, 114.8, 116.4, 122.7, 126.9, 128.6, 129.1, 131.3, 131.7, 137.7, 142.9, 144.1, 151.1; IR ($\nu_{max}$) $cm^{-1}$: 3095 (aromatic C=C-H), 2920 (aliphatic C-H), 1597 (C=N), 1492 (C=C), 1319 (C-N); MS (ESI+): m/z = 516.66 $[M+H]^+$ (Calcd for $C_{25}H_{25}BrClN_3S$: m/z = 514.91 $[M^+]$).

***1-{4-[1-(4-Chlorophenyl)-3-(thiophen-2-yl)-4,5-dihydro-1H-pyrazol-5-yl] phenyl}-4-methylpiperidine(3e)***

Yield 67%; yellow solid; m.p. 143.5-144.2°C; $^1$H NMR (400 MHz, DMSO-$d_6$): $\delta$ 0.92 (3H, d, $J$ = 6.5 Hz, $CH_3$), 1.19 (2H, m, piperidine -$CH_2$- protons), 1.46 (1H, m, piperidine -CH- protons), 1.65 (2H, m, piperidine -$CH_2$- protons), 2.59 (2H, m, piperidine N-$CH_2$- protons), 3.10 (1H, dd, *Jax* = 5.8 Hz, *Jab* = 17.3 Hz, Ha), 3.61 (2H, m, piperidine N-$CH_2$- protons), 3.87 (1H, dd, *Jbx* = 12.0 Hz, *Jab* = 17.3 Hz, Hb), 5.39 (1H, dd, *Jax* = 5.8 Hz, *Jbx* = 12.0 Hz, Hx), 6.86–7.67 (11H, m, Ar-H); $^{13}$C NMR (100 MHz, DMSO-$d_6$): $\delta$ 22.2, 30.6, 33.9, 44.2, 49.0, 49.0, 63.1, 114.7, 116.4, 122.4, 126.9, 128.1, 128.2, 128.3, 129.1, 131.5, 136.0, 143.2, 144.9, 151.1; IR ($\nu_{max}$) $cm^{-1}$: 3066 (aromatic C=C-H), 2920 (aliphatic C-H), 1595 (C=N), 1489 (C=C), 1226 (C-N). MS (ESI+): m/z = 436.73 $[M+H]^+$ (Calcd for $C_{25}H_{26}ClN_3S$: m/z = 435.15 $[M^+]$).

***1-{4-[1-(4-Chlorophenyl)-3-(5-methylthiophen-2-yl)-4,5-dihydro-1H-pyrazol-5-yl]phenyl}-4-methylpiperidine (3f)***

Yield 63%; orange solid; m.p. 138.6-139.3°C; $^1$H NMR (400 MHz, DMSO-$d_6$): $\delta$ 0.93 (3H, d, $J$ = 6.5 Hz, $CH_3$), 1.21 (2H, m, piperidine -$CH_2$- protons), 1.49 (1H, m, piperidine -CH- protons), 1.70 (2H, m, piperidine -$CH_2$- protons), 2.49-2.63 (5H, m, piperidine N-$CH_2$- protons, $CH_3$), 3.04 (1H, dd, *Jax* = 5.9 Hz, *Jab* = 17.3 Hz, Ha), 3.60 (2H, m, piperidine N-$CH_2$- protons), 3.81 (1H, dd, *Jbx* = 12.1 Hz, *Jab* = 17.3 Hz, Hb), 5.36 (1H, dd, *Jax* = 5.8 Hz, *Jbx* = 12.1 Hz, Hx), 6.79–7.49 (10H, m, Ar-H); $^{13}$C NMR (100 MHz, DMSO-$d_6$): $\delta$ 15.7, 22.1, 30.5, 33.7, 44.1, 48.7, 63.0, 113.5, 114.7, 115.7, 116.6, 121.6, 122.2, 126.6, 127.0, 127.3, 128.4, 129.0, 129.2, 131.6, 133.7, 138.5, 141.8, 143.4, 145.0; IR ($\nu_{max}$) $cm^{-1}$: 3047 (aromatic C=C-H), 2910 (aliphatic C-H), 1599 (C=N), 1489 (C=C), 1298 (C-N). MS (ESI+): m/z = 450.75 $[M+H]^+$ (Calcd for $C_{25}H_{26}ClN_3S$: m/z = 449.17 $[M^+]$).

***1-{4-[1-(4-Methoxyphenyl)-3-phenyl-4,5-dihydro-1H-pyrazol-5-yl]phenyl}-4-methylpiperidine (4a)***

Yield 63%; orange solid; m.p. 118.1-118.7°C; $^1$H NMR (400 MHz, DMSO-$d_6$): $\delta$ 0.93 (3H, d, $J$ = 6.5 Hz, $CH_3$), 1.19 (2H, m, piperidine -$CH_2$- protons), 1.46 (1H, m, piperidine -CH- protons), 1.66 (2H, m, piperidine -$CH_2$- protons), 2.60 (2H, m, piperidine N-$CH_2$- protons), 3.03 (1H, dd, *Jax* = 7.3 Hz, *Jab* = 17.4 Hz, Ha), 3.04-3.80 (5H, m, piperidine N-$CH_2$- protons, O-$CH_3$), 3.81 (1H, dd, *Jbx* = 12.0 Hz, *Jab* = 17.3 Hz, Hb), 5.26 (1H, dd, *Jax* = 7.3 Hz, *Jbx* = 12.2 Hz, Hx), 6.78-7.73 (13H, m, Ar-H); $^{13}$C NMR (100 MHz, DMSO-$d_6$): $\delta$ 22.2, 30.6, 34.0, 43.4, 49.1, 49.1, 55.6, 64.2, 114.7, 114.9, 116.4, 125.9, 127.2, 128.7, 129.0, 132.5, 133.0, 139.3, 146.7, 151.0, 153.0; IR ($\nu_{max}$) $cm^{-1}$: 3034 (aromatic C=C-H), 2904 (aliphatic C-H), 1612 (C=N), 1506 (C=C), 1236 (C-N). MS (ESI+): m/z = 426.79 $[M+H]^+$ (Calcd for $C_{28}H_{31}N_3O$: m/z = 425.25 $[M^+]$).

***1-{4-[3-(5-Chlorothiophen-2-yl)-1-(4-methoxyphenyl)-4,5-dihydro-1H-pyrazol-5-yl] phenyl}-4-methylpiperidine (4b)***

Yield 67%; orange solid; m.p. 118.1-118.7°C; $^1$H NMR (400 MHz, DMSO-$d_6$): $\delta$ 0.92 (3H, d, $J$ = 6.5 Hz, $CH_3$), 1.20 (2H, m, piperidine -$CH_2$- protons), 1.48 (1H, m, piperidine -CH- protons), 1.67 (2H, m, piperidine -$CH_2$- protons), 2.63 (2H, m, piperidine N-$CH_2$- protons), 3.02 (1H, dd, *Jax* = 7.2 Hz, *Jab* = 17.2 Hz, Ha), 3.04-3.88 (6H, m, piperidine N-$CH_2$- protons, O-$CH_3$, Hb), 5.30 (1H, dd, *Jax* = 7.2 Hz, *Jbx* = 12.0 Hz, Hx), 6.76-7.15 (10H, m, Ar-H); $^{13}$C NMR (100 MHz, DMSO-$d_6$): $\delta$ 22.1, 30.4, 33.8, 43.4, 55.6, 64.4, 114.8, 115.0, 126.7, 127.3, 128.1, 128.8, 129.5, 135.7, 138.7, 142.9, 153.3; IR ($\nu_{max}$) $cm^{-1}$: 3066 (aromatic C=C-H), 2922 (aliphatic C-H), 1610 (C=N), 1506 (C=C), 1234 (C-N). MS (ESI+): m/z = 466.81 $[M+H]^+$ (Calcd for $C_{26}H_{28}ClN_3OS$: m/z = 465.16 $[M^+]$).

***1-{4-[3-(Furan-2-yl)-1-(4-methoxyphenyl)-4,5-dihydro-1H-pyrazol-5-yl]phenyl}-4-methylpiperidine (4c)***

Yield 68%; red solid; m.p. 149.0-149.6°C; $^1$H NMR (400 MHz, DMSO-$d_6$): $\delta$ 0.91 (3H, d, $J$ = 6.5 Hz, $CH_3$), 1.22 (2H, m, piperidine -$CH_2$- protons), 1.47 (1H, m, piperidine -CH- protons), 1.66 (2H, m, piperidine -$CH_2$- protons), 2.60 (2H, m, piperidine N-$CH_2$- protons), 2.93 (1H, dd, *Jax* = 7.0 Hz, *Jab* = 17.1 Hz, Ha), 2.94-3.83 (6H, m, piperidine N-$CH_2$- protons, O-$CH_3$, Hb), 5.36 (1H, dd, *Jax* = 7.0 Hz, *Jbx* = 12.1 Hz, Hx), 6.60–7.77 (11H, m, Ar-H); $^{13}$C NMR (100 MHz, DMSO-*d6*): $\delta$ 22.1, 33.9, 43.4, 55.6, 55.7, 55.8, 63.6, 110.5, 112.3, 114.2, 114.7, 114.9, 127.2, 138.9, 139.1, 144.3, 148.2, 153.0; IR ($\nu_{max}$) cm$^{-1}$: 3010 (aromatic C=C-H), 2926 (aliphatic C-H), 1610 (C=N), 1504 (C=C), 1236 (C-N). MS (ESI+): m/z = 416.80 $[M+H]^+$ (Calcd for $C_{26}H_{29}N_3O_2$: m/z = 415.23 $[M^+]$).

***1-{4-[3-(5-Bromothiophen-2-yl)-1-(4-methoxyphenyl)-4,5-dihydro-1H-pyrazol-5-yl]phenyl}-4-methylpiperidine (4d)***

Yield 67%; yellow solid; m.p. 124.4-125.1°C; $^1$H NMR (400 MHz, DMSO-$d_6$): $\delta$ 0.92 (3H, d, $J$ = 6.5 Hz, $CH_3$), 1.20 (2H, m, piperidine -$CH_2$- protons), 1.48 (1H, m, piperidine -CH- protons), 1.67 (2H, m, piperidine -$CH_2$- protons), 2.63 (2H, m, piperidine N-$CH_2$- protons), 3.01 (1H, dd, *Jax* = 7.2 Hz, *Jab* = 17.2 Hz, Ha), 3.04-3.77 (6H, m, piperidine N-$CH_2$- protons, O-$CH_3$, Hb), 5.29 (1H, dd, *Jax* = 7.2 Hz, *Jbx* = 12.0 Hz, Hx), 6.77–7.24 (10H, m, Ar-H); $^{13}$C NMR (100 MHz, DMSO-*d6*): $\delta$ 22.2, 30.6, 33.9, 43.5, 49.1, 55.6, 55.8, 64.4, 112.4, 114.7, 115.0, 116.4, 127.2, 127.4, 127.6, 129.5, 131.5, 138.3, 138.7, 142.4, 153.2; IR ($\nu_{max}$) cm$^{-1}$: 3064 (aromatic C=C-H), 2920 (aliphatic C-H), 1610 (C=N), 1504 (C=C), 1232 (C-N). MS (ESI+): m/z = 510.77 $[M+H]^+$ (Calcd for $C_{26}H_{28}BrN_3OS$: m/z = 509.11 $[M^+]$).

***1-{4-[1-(4-Methoxyphenyl)-3-(thiophen-2-yl)-4,5-dihydro-1H-pyrazol-5-yl]phenyl}-4-methylpiperidine (4e)***

Yield 66%; brown solid; m.p. 118.9-119.6°C; $^1$H NMR (400 MHz, DMSO-$d_6$): $\delta$ 0.92 (3H, d, $J$ = 6.5 Hz, $CH_3$), 1.20 (2H, m, piperidine -$CH_2$- protons), 1.48 (1H, m, piperidine -CH- protons), 1.66 (2H, m, piperidine -$CH_2$- protons), 2.60 (2H, t, piperidine N-$CH_2$- protons), 3.04 (1H, dd, *Jax* = 7.3 Hz, *Jab* = 17.1 Hz, Ha), 3.05-3.80 (6H, m, piperidine N-$CH_2$- protons, O-$CH_3$, Hb), 5.25 (1H, dd, *Jax* = 7.3 Hz, *Jbx* = 11.9 Hz, Hx), 6.76–7.56 (11H, m, Ar-H); $^{13}$C NMR (100 MHz, DMSO-*d6*): $\delta$ 22.2, 30.5, 34.0, 44.2, 49.1, 55.6, 64.4, 114.3, 114.7, 114.9, 115.1, 116.4, 127.2, 127.2, 127.3, 128.2, 129.5, 132.2, 136.5, 139.2, 143.3, 151.0, 153.0; IR ($\nu_{max}$) cm$^{-1}$: 3066 (aromatic C=C-H), 2949 (aliphatic C-H), 1610 (C=N), 1506 (C=C), 1236 (C-N). MS (ESI+): m/z = 432.78 $[M+H]^+$ (Calcd for $C_{26}H_{29}N_3OS$: m/z = 431.20 $[M^+]$).

***1-{4-[1-(4-Methoxyphenyl)-3-(5-methylthiophen-2-yl)-4,5-dihydro-1H-pyrazol-5-yl]phenyl}-4-methylpiperidine (4f)***

Yield 66%; brown solid; m.p. 140.2-140.8°C; $^1$H NMR (400 MHz, DMSO-$d_6$): $\delta$ 0.92 (3H, d, $J$ = 6.5 Hz, $CH_3$), 1.18 (2H, m, piperidine -$CH_2$- protons), 1.47 (1H, m, piperidine -CH- protons), 1.67 (2H, m, piperidine -$CH_2$- protons), 2.46-2.59 (5H, m, piperidine N-$CH_2$- protons, $CH_3$), 2.99 (1H, dd, *Jax* = 7.1 Hz, *Jab* = 17.0 Hz, Ha), 3.00-3.90 (6H, m, piperidine N-$CH_2$- protons, O-$CH_3$, Hb), 1.20-3.77 (16H, m, piperidine protons, $CH_3$, -$OCH_3$, Hb), 5.21 (1H, dd, *Jax* = 7.1 Hz, *Jbx* = 11.9 Hz, Hx), 6.76–7.10 (10H, m, Ar-H); $^{13}$C NMR (100 MHz, DMSO-$d_6$): $\delta$ 15.6, 22.2, 30.6, 34.0, 44.0, 49.1, 49.1, 55.6, 64.3, 114.7, 114.8, 116.4, 126. 5, 127.1, 127.4, 132.2, 134.3, 139.3, 141.0, 143.5, 151.0, 152.9; IR ($\nu_{max}$) cm$^{-1}$: 3047 (aromatic C=C-H), 2910 (aliphatic C-H), 1610 (C=N), 1502 (C=C), 1234 (C-N). MS (ESI+): m/z = 446.79 $[M+H]^+$ (Calcd for $C_{27}H_{31}N_3OS$: m/z = 445.22 $[M^+]$).

**Cell viability assay and *in vitro* antiproliferative activity**

L929 healthy fibroblast cells were used in the study to determine whether the synthesized compounds have cytotoxic effects on healthy cells. Fibroblast cells are the most abundant cells in the structure of the connective tissue responsible for the formation of the extracellular matrix and also responsible for the migration, proliferation, and differentiation of cells and have a highly proliferative feature. For this reason, it is used in many biological impact assessment studies (22). MCF-7 (human breast cancer cell line) and A-549 (human lung cancer cell line) cell lines were used in our study to examine the anti-proliferative effects of the synthesized compounds. DMEM containing 2 mm L-glutamine, 10% fetal bovine serum (FBS), and 1% penicillin-streptomycin was used as a cell growth medium. Within the scope of these studies, it was aimed to observe the toxicity of the synthesized compounds in the cells and to find their subtoxic (non-toxic to cells) concentrations. After the substance dissolved in DMSO, dilutions with different concentrations (50, 100, and 200 mM) were prepared by cell culture medium (without exceeding 0,5% DMSO)and tested to calculate 50% inhibitory concentration ($IC_{50}$) values. MTT test was applied

to determine whether the compounds have an antiproliferative effect on the cells. $IC_{50}$ values were calculated using the GraphPad Prism software program 72 hours after the administration of the compounds to the cells (24). The percentage inhibition of synthesized compounds was calculated by using the formula given below:

$$\% \text{ Inhibition} = 100 - \frac{\text{Mean OD of treated cells}}{\text{Mean OD of negative control cells}} \text{ x } 100$$

**Apoptosis assay**

The apoptosis study was performed according to the manufacturer's protocol using the Annexin V-FITC/propidium iodide (PI) apoptosis detection kit (Elabscience). Compounds (200 mM) were treated on cells at 72h. Cells were collected and washed 2 times with PBS and then suspended with binding buffer. Annexin V solution was added to the cell suspension and incubated for 15 min in the dark. Binding buffer and propidium iodide (PI) were then added and the cell suspension was analyzed by flow cytometry (BD Accuri C6 Plus). Annexin V(-)/PI (-) cells are alive, Annexin V (+)/PI (-) cells are early apoptotic, and Annexin V(+)/PI (+) cells are late apoptotic or dead cells. BD CSampler Plus software was used for analysis (23). The histograms show the percentage of apoptosis normalized to those of the untreated cancer cells.

**Fluorescence properties of the compounds**

In order to examine the fluorescence properties of the compounds, the cells were seeded in 6 well plates. After overnight incubation, the synthesized compounds were treated on the cells at a concentration of 100 μM. 24 hours after the treatment of the compounds, the cells were examined under an inverted microscope, and images were taken.

The fluorescence spectra of the compounds which have fluorescence properties were recorded for prepared stock solutions of the compounds in DMSO. Perkin Elmer LS-55 fluorescence spectra were used to record the emission bands of the compounds.

**ADME properties of synthesized compounds**

The SwissADME tool freely was utilized to determine and evaluate the physicochemical and ADME parameters of synthesized compounds (25).

## RESULT AND DISCUSSION

**Chemistry**

Within the scope of this study, in the first step; 4-(4-methyl piperidine-1-yl)benzaldehyde was synthesized with a starting compound carrying a piperidine ring and the 4-fluorobenzaldehyde. In the second step; chalcone derivatives were obtained as a result of base-catalyzed Claisen-Schmidt condensation of 4-(4-methyl piperidine-1-yl)benzaldehyde with different ketone derivatives. In the last step; the unique 2-pyrazoline derivatives were synthesized via cyclo condensation reaction of chalcone derivatives with phenyl/4-chlorophenyl/4-methoxyphenyl hydrazine derivatives. The synthesis method and table of substituents were given in Scheme 1 and Table 1, respectively.

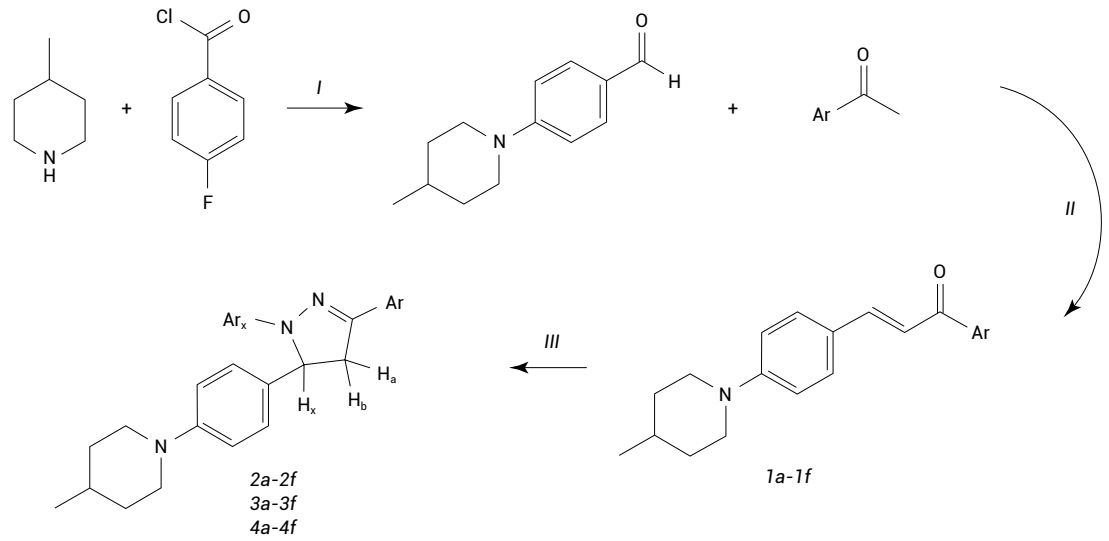


Scheme 1. General synthetic method of target compounds: Reaction and conditions: (I) $K_2CO_3$, DMF, reflux, 10h; (II) Methanol, 50% NaOH, rt; (III) Ethanol, acetic acid, reflux, 15 h.

Table 1. Ar and $Ar_x$ substituents of the compounds.

| Molecule | Ar | $Ar_x$ |
|---|---|---|
| **1a** | Phenyl | - |
| **1b** | 5-Chlorothiophen-2-yl | - |
| **1c** | Furan-2-yl | - |
| **1d** | 5-Bromothiophen-2-yl | - |
| **1e** | Thiophen-2-yl | - |
| **1f** | 5-Methylthiophen-2-yl | - |
| **2a** | Phenyl | Phenyl |
| **2b** | 5-Chlorothiophen-2-yl | Phenyl |
| **2c** | Furan-2-yl | Phenyl |
| **2d** | 5-Bromothiophen-2-yl | Phenyl |
| **2e** | Thiophen-2-yl | Phenyl |
| **2f** | 5-Methylthiophen-2-yl | Phenyl |
| **3a** | Phenyl | 4-Chlorophenyl |
| **3b** | 5-Chlorothiophen-2-yl | 4-Chlorophenyl |
| **3c** | Furan-2-yl | 4-Chlorophenyl |
| **3d** | 5-Bromothiophen-2-yl | 4-Chlorophenyl |
| **3e** | Thiophen-2-yl | 4-Chlorophenyl |
| **3f** | 5-Methylthiophen-2-yl | 4-Chlorophenyl |
| **4a** | Phenyl | 4-Metoxyphenyl |
| **4b** | 5-Chlorothiophen-2-yl | 4-Metoxyphenyl |
| **4c** | Furan-2-yl | 4-Metoxyphenyl |
| **4d** | 5-Bromothiophen-2-yl | 4-Metoxyphenyl |
| **4e** | Thiophen-2-yl | 4-Metoxyphenyl |
| **4f** | 5-Methylthiophen-2-yl | 4-Metoxyphenyl |

**Spectral analysis**

The structures of novel synthesized compounds were illustrated by spectral data including IR, $^{1}$H-NMR, $^{13}$C-NMR, and mass spectrometry. In addition, compounds **2b** and **4b** were confirmed by 2D-NMR (HMBC). IR spectra of chalcone derivatives (**1a-f**) showed the presence of the carbonyl group (C=O) which is conjugated with an olefinic bond (CH=CH) and the C=O stretching band appeared in the range of 1633-1651 $cm^{-1}$. In the IR spectra of the 2-pyrazoline derivatives, C=N bands were observed in the region 1612-1595 $cm^{-1}$. Furthermore, the absence of the carbonyl vibration band of chalcone derivatives confirmed the formation of the pyrazoline ring.

The 2-pyrazoline structure has three characteristic signals of the ABX system due to geminal-vicinal coupling (Figure 1) (26). In $^{1}$H-NMR spectra, $H_a$ protons of pyrazoline structure resonated at 2.93-3.10 ppm as a pair of doublet of doublets with characteristic coupling constant (*J*) values 5.7-7.3 Hz and 17.0-17.5 Hz for all compounds. $H_b$ proton signals of compounds **2a-f** and **3a-f** were observed as a doublet of doublets with a coupling constant of 11.9-12.1 Hz and 17.0-17.5 Hz at 3.76-3.87 ppm. $H_b$ proton signals of compounds **4a-f** were observed as a multiplet signal at 3.10-3.84 ppm due to methyl protons of the methoxy group (-$OCH_3$). The signal of methine proton ($H_x$) at the 5th position of the pyrazoline ring was observed as a doublet of doublets at 5.21-5.41 ppm with a coupling constant of 5.7-7.3 Hz and 11.9-12.2 Hz. All the other aromatic and aliphatic protons were observed in the expected regions.

In the $^{13}$C-NMR spectra, chemical shift values confirmed the property of the pyrazoline ring. The $C_3$, $C_4$, and $C_5$ carbon signals of the pyrazoline scaffold were observed at 144.68-153.24 ppm, 43.35-44.29 ppm, and 62.57-64.46 ppm, respectively. The carbon signal of the methyl group of the piperidine ring was observed at 22.19-22.24 ppm. The spectrums of compounds **2f**, **3f** and **4f** showed carbon

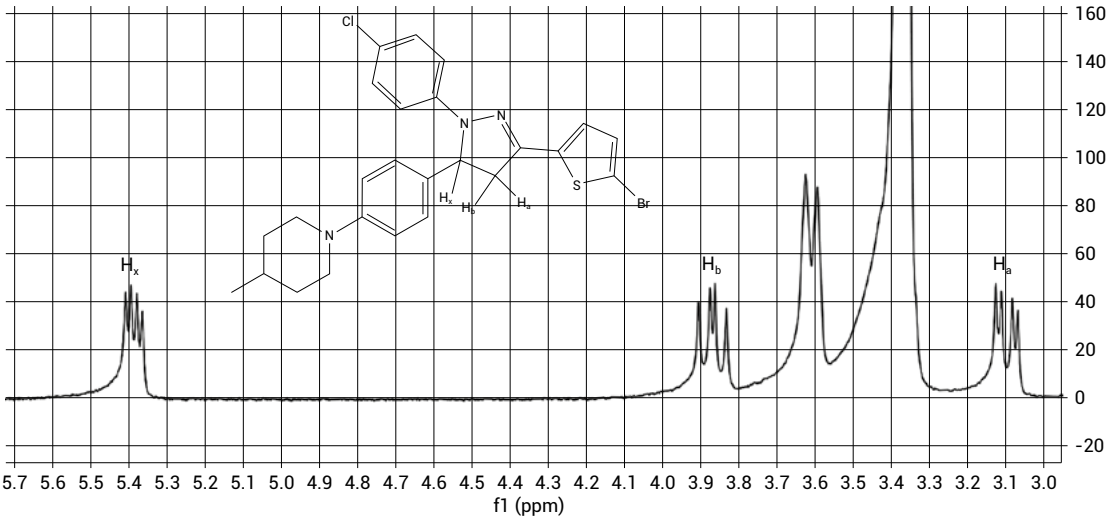


Figure 1. $^{1}$H-NMR spectra of compound 3d as an example. The part of spectra shows that the signals of $H_x$, $H_{a,}$ and $H_b$ protons were observed as a doublet of doublets.

signals of methyl substitution of the thiophene ring at 15.68-15.70 ppm.

HMBC (heteronuclear multiple bond coherence) spectroscopy plays a key role to explain the correlations of $^{13}$C and $^{1}$H atoms through two, three, or sometimes four bonds. HMBC was used to confirm the structure of the molecule. HMBC spectrum of **2b** shows correlations of H-7 with C-1, C-2 and C-6, H-14 with C-10 and C-12, H-10 and H-12 with C-14. Moreover, satellite signals of the H-7 methyl protons, being linked to directly the C-7 carbon atom, were observed in the spectrum. Further, HMBC correlations between aromatic protons and aromatic carbon atoms were obtained. The HMBC spectrum of **4b** showed correlations between H-7 with C-1, C-2 and C-6, H-31 with C-22, and H-3 and H-5 with C-8. The satellite signals of the H-31 methyl protons, being connected with directly the C-31 carbon atom, were observed (Figure 2).

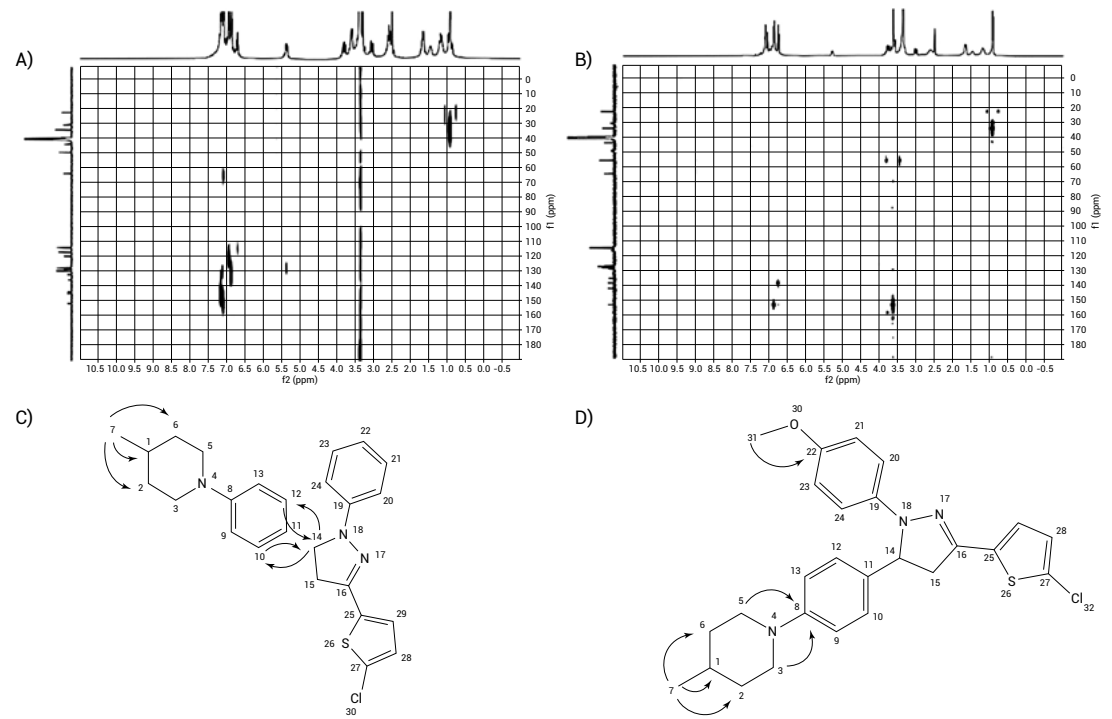


Figure 2. A) HMBC spectrum of compound 2b. B) HMBC spectrum of compound 4b. C) Correlations between protons and carbon atoms in compound 2b. D) Correlations between protons and carbon atoms in compound 4b.

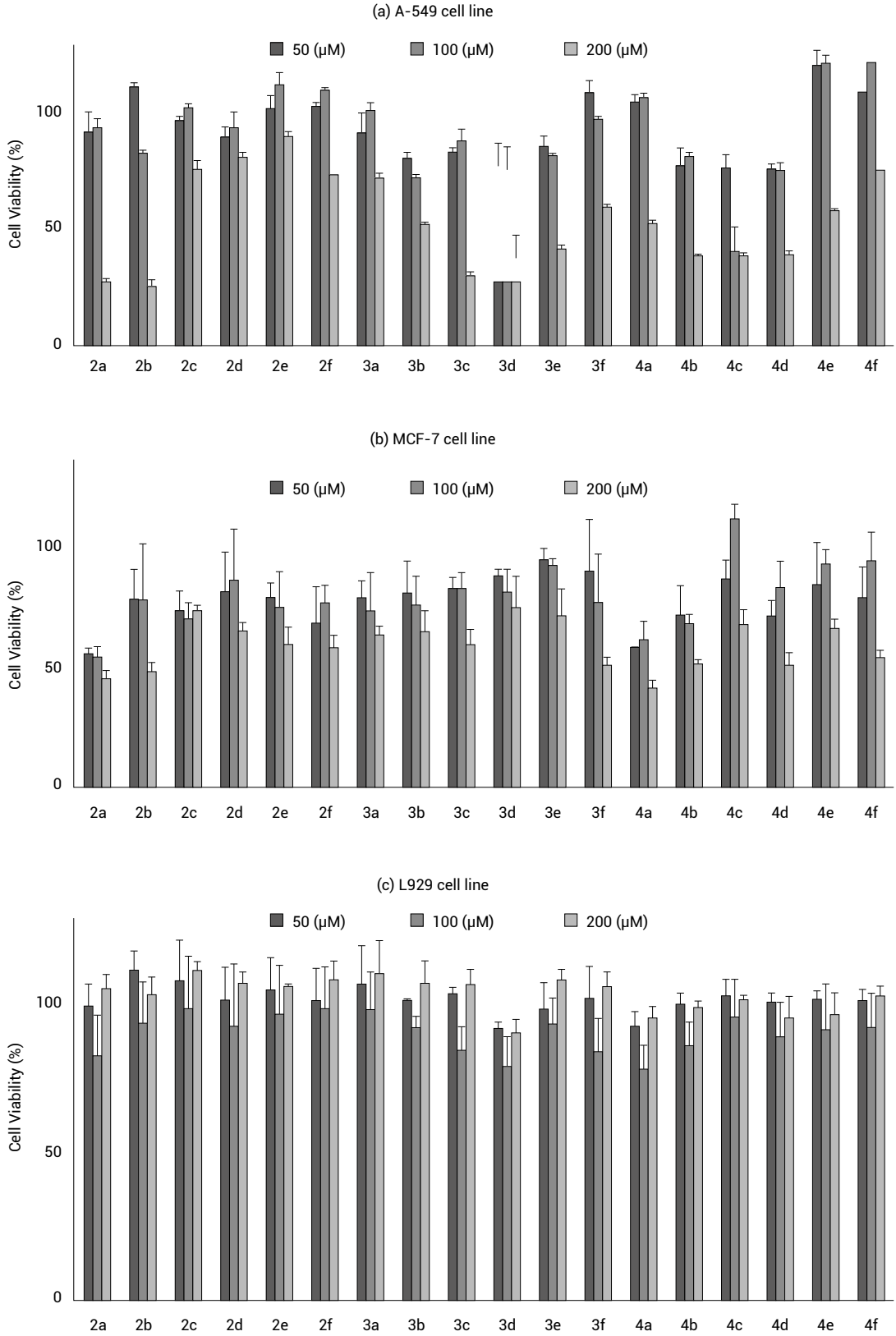


Figure 3. Graphical representation of the cytotoxic effect of the 2-pyrazoline derivatives as cell viability percentages A) Antiproliferative activity of the synthesized 2-pyrazoline compounds on A-549 cell lines. B) Antiproliferative activity of the synthesized 2-pyrazoline compounds on MCF-7 cell lines C) Cytotoxic effect of the synthesized 2-pyrazoline compounds on L929 cell lines.

Additionally, the mass spectrometry data of synthesized compounds were consistent with their depicted structures. Spectra data of novel synthesized compounds were maintained in the supplementary materials.

## Biology

### Antiproliferative activity

By performing an MTT assay, newly synthesized 2-pyrazoline compounds were screened to evaluate their antiproliferative activity according to ISO 10993-5 protocol. A-549 (human lung adenocarcinoma) and MCF-7 (human breast adenocarcinoma) were used to determine their antiproliferative effect and L929 (mouse fibroblast) cell lines were used to examine cytotoxic effects in healthy cells. The compounds were tested at three doses (50 mM, 100 mM, and 200 mM) against the cell lines. Doxorubicin was used as a positive control. The antiproliferative activities of compounds are presented in Figure 3 as cell viability percentages.

From the obtained data, it was found that the compounds showed a dose-dependent effect and inhibited the proliferation of the carcinoma cell lines in the range between 25 and 90% in concentrations of 100-200 mM. Considering the percentages of the cell proliferation inhibition of compounds **2a**, **2b,** and **4a**, it was noticed that these compounds showed the most cytotoxic activity in MCF-7 cell lines at 200 mM. The proliferation of the A-549 cell lines treated with compounds **2a**, **2b**, **3c**, **4b**, **4c,** and **4d** was decreased, and statistically significant as compared to the non-treated control cell lines. $IC_{50}$ values of effective compounds were given in Table 2.

The antiproliferative effect on lung carcinoma of the synthesized compounds was higher than breast carcinoma. According to obtained results from cytotoxic activity studies using L929 cell lines, it was observed that the compounds did not cause a cytotoxic effect on fibroblast cells. It is seen that the cell viability values of the compounds are close to the negative control group.

### Apoptosis assay

The active synthesized compounds were investigated to determine whether their cytotoxic activity was attributed to apoptosis or necrosis. Flow cytometry assay was utilized to evaluate of cell death mechanism. The obtained results were given in Figure 4. The results were helpful to examine the differentiation between living (LL), early apoptotic (LR), late apoptotic (UR), and necrotic (UL) cells.

As given in flow cytometry charts, cell deaths were mostly induced by apoptosis. After treatment of the A-549 cell line with compounds **2a**, **2b**, **3c,** and **4d**, a decrease in the percentage of live cells was observed. Moreover, 95.7% and 85.5% of dead cells treated with **2a** and **3c** were in the late apoptotic phase, respectively. A decrease in the percentage of live MCF-7 cells treated with compounds **2b**, **3c**, **4a,** and **4d** was observed. It was found that the death pathway was apoptotic and it was similar to the effect of compounds in the A-549 cell line. Based on the MTT assay and flow cytometry test, the examined compounds can be considered apoptotic inducers.

### Fluorescence properties

Fluorescence property has great importance in life science applications such as in microscopy to localize and quantify biomolecules, in-microplate-based assays to quantify molecules, and even enzymatic activities (27). Novel 2-pyrazoline derivatives

Table 2. $IC_{50}$ values of the effective compounds on MCF-7 and A-549 cell lines.

| IC50 Values | | |
|---|---|---|
| Compounds | MCF-7 | A-549 |
| **2a** | 146.3± 38.9 µM | 172.8 ± 2.7 µM |
| **2b** | 187.3 ± 18.8 µM | 145.6 ± 6.7 µM |
| **3c** | - | 173.6 ± 3.4 µM |
| **4a** | 166.1 ± 7.7 µM | - |
| **4b** | - | 180.4 ± 2.5 µM |
| **4c** | - | 81.1 ± 4.0 µM |
| **4d** | - | 171.1 ±17.9 µM |
| **Doxorubicin** | 174.5 nM | 273.7 nM |

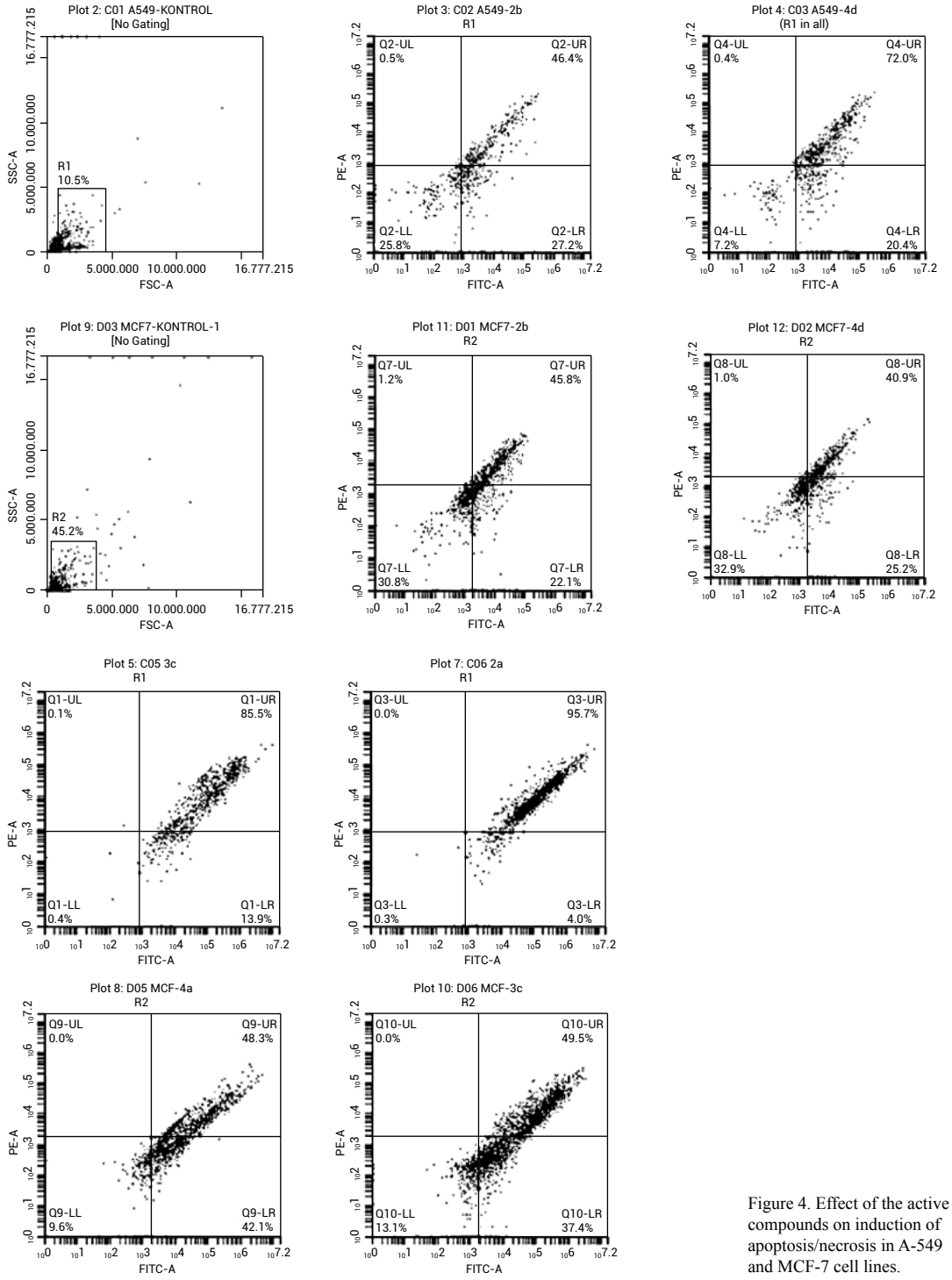


Figure 4. Effect of the active compounds on induction of apoptosis/necrosis in A-549 and MCF-7 cell lines.

were synthesized and examined to imagine their fluorescence property. When the compounds were examined in fluorescence microscopy, it was observed that compounds **4b**, **4d**, **4e,** and **4f** showed fluorescence properties, completely penetrated cells, and their localization site is seen as cytoplasmic (Figure 5).

The fluorescence spectra of the compounds **4b**, **4d**, **4e,** and **4f** were recorded using excitation wavelengths of 410 nm, 460 nm, 420 nm, and 400 nm, respectively, with an excitation/emission slit width of 5/10 nm. The spectrums were shown in Figure 6. The maximal emission wavelength of the compounds **4b**, **4d**, **4e,** and **4f** was

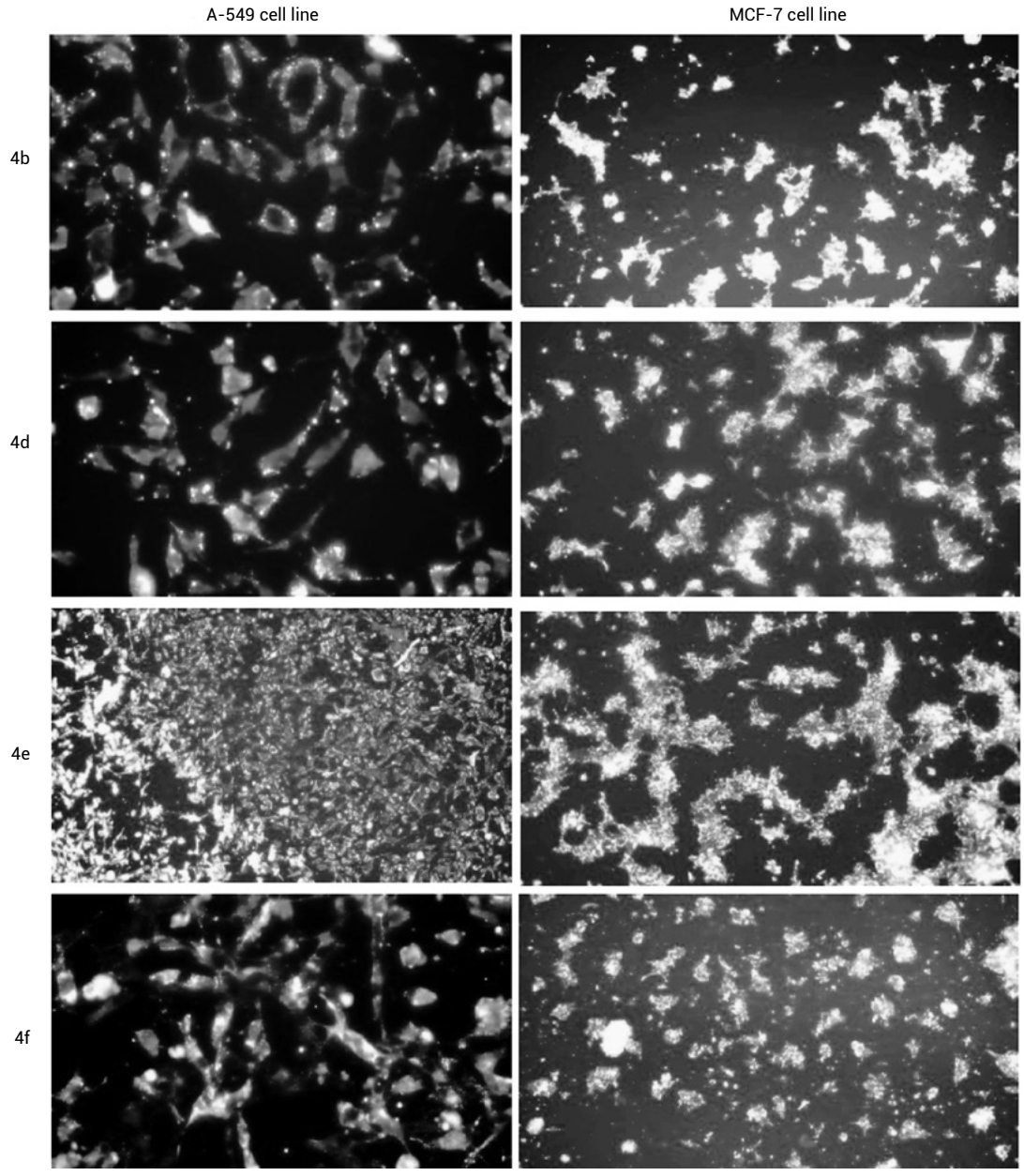


Figure 5. The images show that examined compounds by fluorescence microscopy have fluorescence activity.

observed at 537 nm, 566 nm, 514 nm, and 500 nm, respectively.

These compounds have optimal properties such as being non-toxic, having eligible pharmacokinetic characteristics which a fluorophore should have, and emitting light at the appropriate wavelength. Considering the advantages and importance of fluorescence properties in medicine, this data shows promising results for the synthesis and development of new fluorophores that could be used in medicine or for future studies on whether the compounds could be used in this field.

**Prediction of ADME properties**

The primary procedure in drug development is the selection of effective potential drug candidate compounds that can pass into the active site of the body (28). Absorption, distribution, metabolism, and extraction (ADME) properties have an important role in the development of compounds that could be drug candidates. Considering that 40 percent of drug development failures are due to pharmacokinetic properties, the development of these parameters will save time and money. Although it is not used as a stand-alone identifier

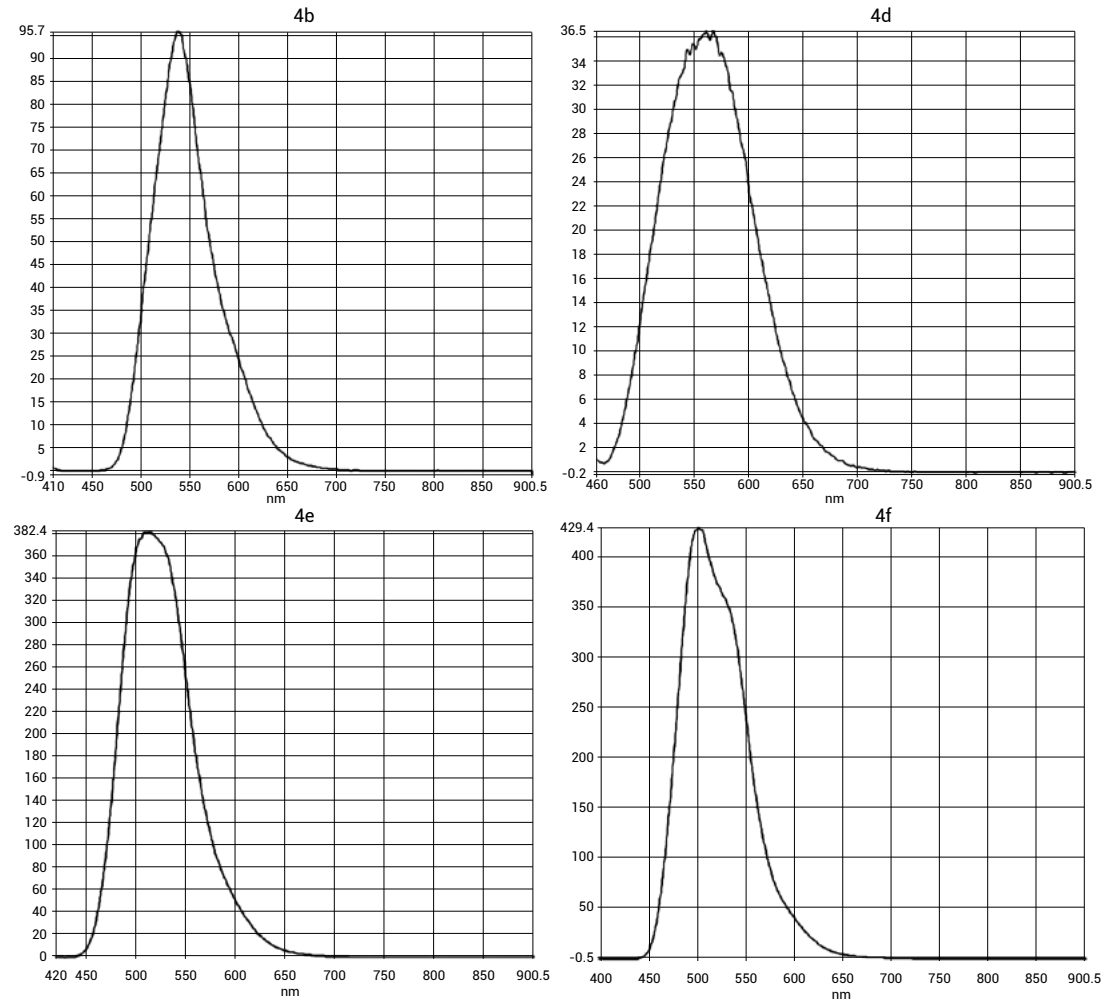


Figure 6. Fluorescence spectra for compounds 4b, 4d, 4e, and 4f in DMSO.

due to the complexity of the ADME process, it provides a great advantage for drug optimization (29). SwissADME contains the most appropriate calculation methods together to evaluate the physicochemical and pharmacokinetic parameters of small molecules (30). The SwissADME program is a free web tool used to calculate the ADME properties of molecules, such as the permeability of the blood-brain barrier system, and their physicochemical properties, including the Lipinski and Veber rules. Water solubility and lipophilicity properties are used for absorption calculations of compounds. LogS descriptors of SwissADME are used to evaluate the water solubility of drug candidates. Lipophilicity which is calculated using consensus LogP is the logarithmic value of the n-octanol/water partition coefficient and it is closely related to the distribution of different tissues and organs, and membrane permeability. Distribution is calculated using glycoprotein P (P-gp) substrate and permeation of the blood-brain barrier system (BBB). The BBB system is a complex structure that allocates the central nervous system (CNS) and the peripheral tissue. It ensures that toxins and metabolites in the brain are cleared from the brain to the blood. It also controls the process of transfer of materials between the blood and the brain. The BOILED-Egg graph is used to appreciate the permeation of the BBB system. This method functions by predicting the polarity (TPSA) and lipophilicity (logP) of the molecules. Yellow Boiled Egg denotes indicates that the molecules permeate through the blood-brain barrier (BBB) passively, while the white part of the Boiled Egg indicates that the molecules are passively absorbed by the gastrointestinal system. P-gp is an ATP-dependent pump and helps molecules predicted to be effluated from CNS. Blue dots in the BOILED-Egg graph show molecules which are flow out by P-gp (31, 32). BOILED-Egg diagram obtained from the SwissADME website of

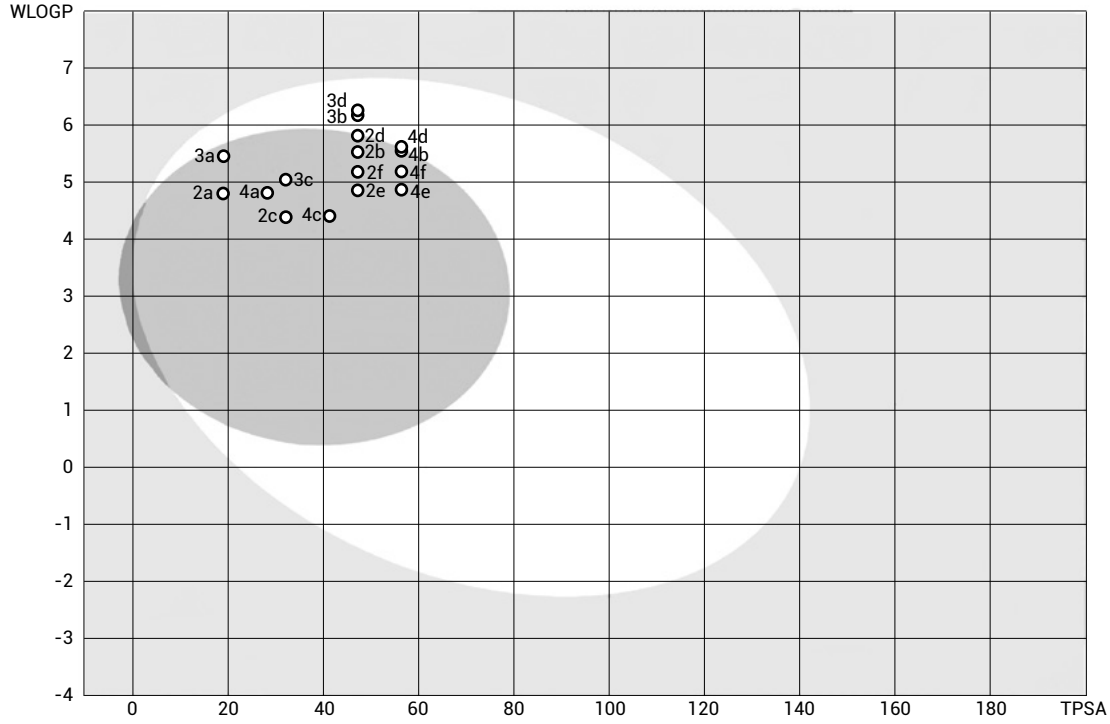


Figure 7. BOILED-Egg graph of the synthesized compounds.

prepared compounds given in Figure 7. According to the graph, the resulting output showed that all tested compounds have BBB penetration except **3b, 3d,** and **4d**.

Table 3. Calculated ADME and physicochemical parameters of synthesized compounds *via* the SwissADME tool.

| Molecule | MW | Rotatable bonds | H-bond acceptors | H-bond donors | TPSA | MLOGP | Log S | GI absorption | BBB permeant | Pgp substrate |
|---|---|---|---|---|---|---|---|---|---|---|
| **2a** | 395.54 | 4 | 1 | 0 | 18.84 | 5.11 | -6.52 | High | Yes | Yes |
| **2b** | 436.01 | 4 | 1 | 0 | 47.08 | 5.21 | -7.36 | High | Yes | Yes |
| **2c** | 385.50 | 4 | 2 | 0 | 31.98 | 3.89 | -6.07 | High | Yes | Yes |
| **2d** | 480.46 | 4 | 1 | 0 | 47.08 | 5.31 | -7.68 | High | Yes | Yes |
| **2e** | 401.57 | 4 | 1 | 0 | 47.08 | 4.74 | -6.56 | High | Yes | Yes |
| **2f** | 415.59 | 4 | 1 | 0 | 47.08 | 4.94 | -6.88 | High | Yes | Yes |
| **3a** | 429.98 | 4 | 1 | 0 | 18.84 | 5.58 | -7.12 | High | Yes | Yes |
| **3b** | 470.46 | 4 | 1 | 0 | 47.08 | 5.68 | -7.96 | High | No | Yes |
| **3c** | 419.95 | 4 | 2 | 0 | 31.98 | 4.36 | -6.66 | High | Yes | Yes |
| **3d** | 514.91 | 4 | 1 | 0 | 47.08 | 5.78 | -8.27 | High | No | Yes |
| **3e** | 436.01 | 4 | 1 | 0 | 47.08 | 5.21 | -7.15 | High | Yes | Yes |
| **3f** | 450.04 | 4 | 1 | 0 | 47.08 | 5.41 | -7.48 | High | Yes | Yes |
| **4a** | 425.57 | 5 | 2 | 0 | 28.07 | 4.72 | -6.60 | High | Yes | Yes |
| **4b** | 466.04 | 5 | 2 | 0 | 56.31 | 4.83 | -7.44 | High | Yes | Yes |
| **4c** | 415.53 | 5 | 3 | 0 | 41.21 | 3.53 | -6.15 | High | Yes | Yes |
| **4d** | 510.49 | 5 | 2 | 0 | 56.31 | 4.93 | -7.76 | High | No | Yes |
| **4e** | 431.59 | 5 | 2 | 0 | 56.31 | 4.36 | -6.63 | High | Yes | Yes |
| **4f** | 445.62 | 5 | 2 | 0 | 56.31 | 4.56 | -6.96 | High | Yes | Yes |

In this study, the evaluated physicochemical parameters are molecular weight (MW), lipophilicity (MLogP), H-bonding donors (HBD), H-bonding acceptors (HBA), rotatable bonds (RB), and topological surface area (TPSA). Selected druglike-ness properties using Lipinski and Veber Rules are predicted via the SwissADME tool. Their rules are listed as follows:

– Lipinski Rules: MW ≤ 500; MLogP ≤ 4.15; HBA ≤ 10; HBD ≤ 5 (33);
– RB ≤ 10; TPSA ≤ 140 (34).

Table 3 aimed to show the important ADME and physicochemical parameters of the synthesized compounds which were calculated by using the SwissADME website tool. According to Lipinski Rules, there should not be more than one violation of the above parameters. Except for **3d** and **4d**, all compounds did not violate mentioned parameters more than once.

## CONCLUSION

In this article, novel 2-pyrazolines were synthesized *via* cyclo condensation reaction between chalcone and hydrazine derivatives. The synthesized compounds were characterized by spectral techniques namely IR, $^{1}$H-NMR, $^{13}$C-NMR, and MS, further confirmed by HMBC spectra for compounds **2b** and **4b**.

All compounds were investigated against A-549 and MCF-7 cell lines and the cytotoxic activities of the compounds were examined in L-929 cell lines. Furthermore, an Annexin V-FITC apoptosis assay was carried out to assess the apoptotic effects of the compounds in breast and lung cancer cells by using flow cytometry. Considering the MTT and apoptosis assay, none of all compounds showed a cytotoxic effect in healthy cells and the compounds which have antiproliferative effects in cancer cell lines can be considered apoptotic inducers.

The fluorescence properties of the compounds were examined by fluorescence microscopy. Based on the results, compounds **4b**, **4d**, **4e,** and **4f** showed fluorescence properties. The obtained data present promising results to utilize fluorescence imaging in cells owing to their fluorescence properties and the nontoxic effects of the compounds in healthy cells.

### Acknowledgments

This work was supported by the Scientific and Technological Research Council of Turkey (TÜBİTAK). Grant No: 221S850.

### Conflicts of interest

The authors declare no conflict of interest.

## REFERENCES

1. Specht E.A., Braselmann E., Palmer A.E.: Annu. Rev. Physiol. 79, 93 (2017).
2. Wagh S., Maslivetc A., Clair J.L., Kornienko A.: ChemBioChem 22, 3109 (2021).
3. Zhu H., Fan J., Du J., Peng X.: Acc. Chem. Res. 49, 2115 (2016).
4. He X., Cao X., Tian X., Bai Y.: Microchem. J. 166, 106135 (2021).
5. Rani M., Mohamad Y.: J. Saudi Chem. Soc. 18, 411 (2014).
6. Emayavaramban M., Santhi N., Gopi C., Manivannan C., Raguraman A.: Int. Lett. Chem. 14, 172 (2013).
7. Altintop M.D., Özdemir A., Turan-Zitouni G., Ilgin S., Atli Ö., et al.: Eur. J. Med. Chem. 92, 342 (2015).
8. Copp F.C., Islip P.J., Tateson J.E.: Biochem. Pharmacol. 33, 339 (1984).
9. Tok F., Abas I., Çevik O., Koçyiğit-Kaymakçıoğlu B.: Bioorg. Chem. 102, 104063 (2020).
10. Özdemir Z., Kandilci H.B., Gümüşel B., Çaliş Ü., Bilgin AA.: Eur. J. Med. Chem. 42, 373 (2007).
11. Kaplancikli ZA., Turan-Zitouni G., Özdemir A., Devrim Can Ö., Chevallet P.: Eur. J. Med. Chem. 44, 2606 (2009).
12. Kumar A., Varadaraj B.G., Singla R.K.: Bull. Fac. Pharm. Cairo Univ. 51, 167 (2013).
13. Manna F., Chimentil F., Bolascol A., Cenicolaz M.L., Amico M.D., et al.: Eur. J. Med. Chem. 27, 633 (1992).
14. Şenol A.V., Bayrak Ç., Menzek A., Onganer Y., Yaka N.: J. Mol. Struct. 1214, 128213 (2020).
15. Zhang Y., Chen Y., Xue Q., Yang Y., Guo H., Xue J.: Inorg. Chem. Commun. 129, 108612 (2021).
16. Han X., Wang Y., Huang Y., Wang X., Choo J., Chen L.: J. Hazard. Mater. 431, 128527 (2022).
17. Zhang Y., Dong Y., Yang Y., Guo H., Cao B., Sun S.: Spectrochim. Acta A Mol. Biomol. Spectrosc. 177, 539 (2017).
18. Wagner A., Schellhammer C., Petersen S.: Angew. Chem. 5, 699 (1966).
19. Osmaniye D., Levent S., Karaduman AB., Ilgın S., Özkay Y., Kaplancıklı ZA.: Molecules 23, 1054 (2018).

20. Elkhalifa D., Siddique B., Qusa M., Cyprian F.S., El-Sayed K., et al.: Eur. J. Med. Chem. 187, 111954 (2020).
21. Tala S.D., Vekariya P.B., Ghetiya R.M., Dodiya B.L., Joshi H.S.: Indian J. Chem. Sect. B. 52, 807 (2013).
22. Lopes V.R., Schmidtke M., Fernandes M.H., Martins R., Vasconcelos V.: Toxicol. In Vitro 25, 944 (2011).
23. Alagöz M.A., Karakurt A., Hepokur C., Şalva E., Önkol T., et al.: Processes 9, 16 pages (2021).
24. El-Naggar M., Almahli H., İbrahim H., Eldehna W., Abdel-Aziz H.: Molecules 23, 1459 (2018).
25. Daina A., Michielin O., Zoete V.: Sci. Rep. 7, 42717 (2017).
26. Sever B., Altıntop M.D., Rodwan M., Özdemir A., Otsuka M., et al.: Eur. J. Med. Chem. 182, 111648 (2019).
27. Lakowicz J.: Principles of Fluorescence Spectroscopy, 3rd. ed., University of Maryland School of Medicine Baltimore, Maryland (2006).
28. Murugavel S., Deepa S., Ravikumar C., Ranganathan R., Alagusundaram P.: J. Mol. Struct. 1222, 128961 (2020).
29. Duran Iturbide N.A., Diaz-Eufracio B.I., Medina-Franco J.L.: ACS Omega 5, 16076 (2020).
30. Dominguez-Villa F.X., Duran-Iturbide N.A., Avila-Zarraga J.G.: Bioorg. Chem. 106, 104497 (2021).
31. Daina A., Zoete V.: ChemMedChem 11, 1117 (2016).
32. Małkiewicz M.A., Szarmach A., Sabisz A.: J. Neuroinflammation 16, 15 (2019).
33. Lipinski C., Lombardo F., Dominy B., Feeney P.: Adv. Drug Deliv. Rev. 23, 3 (1997).
34. Veber D., Johnson S.R., Cheng H., Smith B., Ward K., Kopple K.: J. Med. Chem., 45, 2615 (2002).